The total failures of GPS functioning caused by the powerful solar radio burst on December 13, 2006

E. L. Afraimovich, V. V. Demyanov, and G. Ya. Smolkov

Institute of Solar-Terrestrial Physics, the Russian Academy of Sciences, the Siberian Branch, 664033, Irkutsk, Russia

We investigated failures in the GPS performance produced by extremely dense solar radio burst fluxes associated with the intense (X3.4 in GOES classification) solar flare and Halo CME recorded by SOHO/LASCO on December 13, 2006. According to substantial experimental evidence, high-precision GPS positioning on the entire sunlit side of the Earth was partially disrupted for more than 12–15 min; the high level of GPS slips resulted from the wideband solar radio noise emission. Our results are in agreement with the data obtained recently for the extreme solar radio burst on December 6, 2006, and provide a sound basis for revising the role of space weather factors in the functioning of state-of-the-art satellite systems and for taking a more thorough account of these factors in their development and operation.
Key words: Solar flares, solar radio emission, GPS, GLONASS, GALILEO.

1. Introduction

Strong solar activity observed on December 6 and 13, 2006; i.e., during the solar cycle 23 minimum, was absolutely unexpected. Its study and analyses of the consequences for the space environment are not complete yet. This kind of solar activity is of great interest not only to astronomers and radio astronomers, but to other scientists and engineers, as well. The broadband solar radio emission following the flare exceeded powerful solar radio bursts in all known flares by at least two orders of magnitude (Cerruti *et al.*, 2006a, b; Carrano *et al.*, 2007; Carrano and Bridgwood, 2008; Gary, 2008).

The powerful solar radio burst (SRB) on December 6, 2006, led to failures in the functioning of wideband satellite radio systems including the GPS. The functioning failures and deep damping of GPS signals were registered at certain standard GPS receivers and specialized monitors of ionospheric scintillations in the *L* range (Cerruti *et al.*, 2006a, b; Carrano *et al.*, 2007; Carrano and Bridgwood, 2008; Kintner, 2008). However, worldwide failures of the GPS due to extreme solar activity in December 2006 are still a matter of debate. Meanwhile, this problem is of doubtless scientific and practical interest as regards to the estimation of the space weather effect on the functioning of one of the most powerful and reliable satellite systems considered practically impregnable. Using data from the global network of dual-frequency GPS receivers, Afraimovich *et al.* (2007) found significant evidence that the high-precision GPS positioning on the entire sunlit side of the Earth was paralyzed for more than 10 minutes on December 6, 2006.

There are many published papers regarding the GPS fail-

ure during the 2006 December 6 SRB (see References). But we do not know any publications on the GPS failure during the 2006 December 13 powerful SRB, although the radio flux $F(t)$ was strong enough for both bursts. In this study, we investigate global failures of the GPS performance due to the 2006 December 13 SRB.

2. The Solar Radio Bursts on 13 December 2006 (Concise Description)

Complex, and especially large, microwave bursts were recorded from 02:21 to 04:37 UT, exhibiting weakening with time. A type II burst (02:27–02:44 UT) was followed by a type IV radio burst that ended at 10:12 UT (signatures of wideband solar radio noise emission and disturbances of the solar corona). This radio emission is associated with X-type flare and Halo CME. The latter commenced at 02:18:30 UT (first seen by the LASCO C2 at 02:54 UT and by the LASCO C3 at 03:18 UT; the C3 occulting disk was fully surrounded by 03:42 UT, the mean plane-of-the-sky speed was ∼1440–1800 km/sec). The events with MHD fast-mode shock wave (type II) and plasmoid ejection (Halo CME) are confirmed by observations with the EUV Imaging Spectrometer on-board the Hinode satellite (Asai *et al.*, 2008). Such radio emission was associated with an X-type flare, proton storms, and Halo CME. The said events started and developed at different time intervals and stages of the flare and at different heights in the solar atmosphere.

The flare occurred at the apparent collision site between the large opposite polarities of the umbral magnetic field of AR 10930. The polarity inversion line at the collision site became very complicated and unsteady due to highly sheared magnetic fields caused by the rotation and W-to-E motion of emerging fluxes. The fine structure of magnetic fields at the flare site changed with time: some parts of the complicated polarity inversion line disappeared, and then the azimuthal angle of the magnetic fields changed
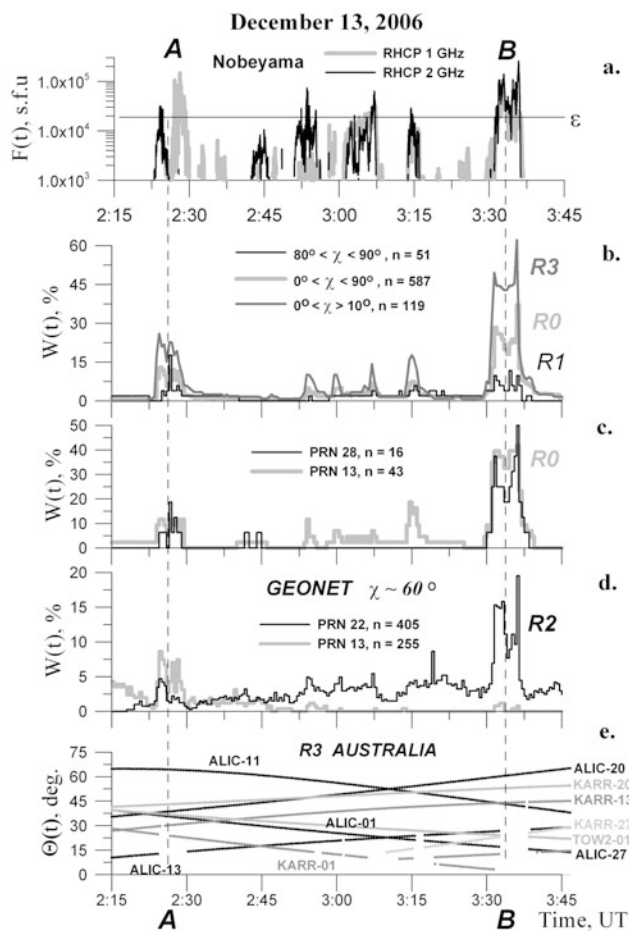
Fig. 1. The relative number of GPS sites $W(t)$ where the 30-s count omissions were observed during December 13, 2006, solar radio bursts: (a) the flux $F(t)$ of the RHCP radio emission observed by the Nobeyama Radio Polarimeters at 1 GHz and at 2 GHz; thick gray line and black line, respectively; logarithmic scale. The vertical dashed lines correspond to the centre of time intervals A and B. About the marks A and B look in the text. (b) region R_3, Australia; region R_0, GPS world network, and region R_1, Western Asia, gray line, thick gray line and black line, respectively, all PRN; (c) region R_0, GPS world network, PRN 13 and 28, thick gray line and black line, respectively; (d) region R_2, GEONET, PRN 13 and 22, thick gray line and black line, respectively; (e) time dependences of elevation angle $\theta(t)$ for different PRN and selected GPS sites KARR, ALIC, TOW2, region R_3, Australia (dots); empty time intervals correspond to the count omissions.

by $\sim 90°$ in those areas, becoming more spatially uniform within the collision site (Kubo *et al.*, 2007; Su *et al.*, 2007). In such circumstances the Right Hand Circular Polarization (RHCP) of microwave bursts can only be registered in certain intervals of the flare time. This was clearly confirmed by observations of total fluxes and circular polarity at the Nobeyama Radio Polarimeters (see Fig. 1(a)) and fixed-frequency observations of total fluxes in other observatories (RSTN Learmonth, Palehua, http://www.ngdc.noaa.gov/stp/SOLAR/ftpsolarradio.html). Moreover, the circular polarity of microwave bursts during the X3.4 flare in December 2006 could also change due to the reversal of the circular polarity sign when the radio emission was propagating across a fragmented magnetic field.

This study is focused on the microwave band of two GPS frequencies ($f_1 = 1575.42$ MHz and $f_2 = 1227.60$ MHz) at 2:20–2:28 UT (corresponding to the type II radio burst) and 3:30–3:38 UT (corresponding to the type IV radio burst). Klobuchar *et al.* (1999) predicted that solar radio bursts could affect GPS performance if a solar flux was sufficiently large in the L band frequency range and had a RHCP—to which polarization GPS antennas are receptive. Therefore it is important first to know data of solar radio flux with RHCP, especially near the auxiliary GPS frequency f_2 (see below Section 5.2).

Data from the Nobeyama Radio Polarimeters (http://solar.nro.nao.ac.jp/norp/html/event/20061213_0247/) show that the RHCP solar radio emission on December 13, 2006 exceeded $1.47 \cdot 10^5$ sfu at 1 GHz at 02:28:09 UT, exceeding $2.57 \cdot 10^5$ sfu at 2 GHz at 03:35:51 UT (Fig. 1(a), thick gray line and black line, respectively). The sharp impulses of the solar radio flux can be noted in the first interval, 02:20 to 02:28 UT (symbol A), and in the second interval, 03:30 to 03:38 UT (symbol B). The vertical dashed lines correspond to the centre of time intervals A and B.

3. Method for GPS Data Processing

We use the GLOBDET software developed at the ISTP SB RAS to treat GPS data from the global network of dual-frequency receivers (Afraimovich *et al.*, 2000; Afraimovich, 2000). Our database of the GPS network's RINEX files includes data from over 1500 GPS sites (http://sopac.ucsd.edu/other/services.html). We also complement data from the Japanese GPS network GEONET (about 1225 sites in all) (ftp://terras.gsi.go.jp/data/GPS_products/). At present, it is the largest regional GPS network in the world.

Figure 2 presents the geometry of the global network of GPS receivers in the Earth sunlit side ((a), (b), gray circles) and GEONET geometry ((b), black triangles) on December 13, 2006. The names of the sites are not given, for reasons of space. It is clear that the level of solar noise interference depends on the Sun zenith angle χ (Carrano *et al.*, 2007). We have examined this dependence. The rectangles mark different regions (R_0–R_3) with different zenith angles χ. Asterisks show the location of sunlit points for December 13, 2006, at 02:30 and 03:30 UT. The bold triangles on Fig. 2 (region R_3, Australia) mark selected GPS sites KARR, ALIC, TOW2.

In order to estimate the GPS performance we used different methods for processing RINEX files described by Afraimovich *et al.* (2002). For all n lines of sight (LOS) between the GPS world network receivers and satellites we calculate the relative number of GPS sites $W(t)\%$, where the 30-s count omission for GPS satellites with their pseudo random noise (PRN) code number (Hofmann-Wellenhof *et al.*, 1992) was simultaneously observed at two GPS frequencies f_1 and f_2.

In addition, for all LOSs between GEONET/GPS receivers and PRN, we calculated the relative density $Q(t)\%$ of measurement slips of main GPS-signal parameters: L_1, L_2 are the phase delay, and P_1, P_2 the group delay for f_1 and f_2, respectively. A measurement slip was registered when the current 30-s count of corresponding GPS parameters equaled zero or the current 30-s count of all parameters
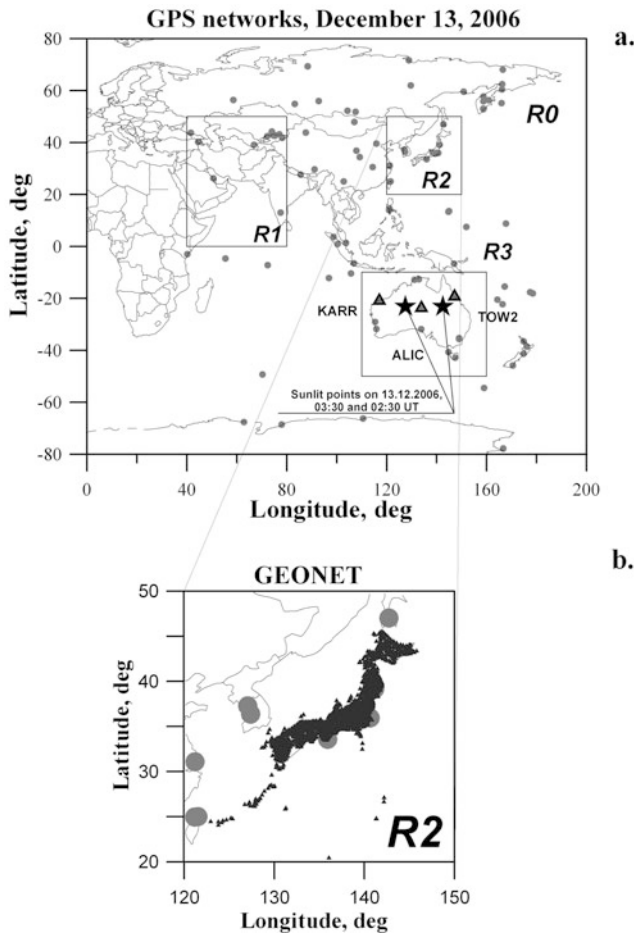
Fig. 2. The geometry of global network of GPS receivers in sunlit side of the Earth ((a), (b), gray circles) and GEONET geometry in Japan ((b), black triangles). The names of the sites are not given for reasons of space. The rectangles mark different region (R_0–R_3) with different Sun zenith angles χ. Stars at Australia map R_3 show the location of the sunlit points for December 13, 2006, on 02:30 and 03:30 UT; the bold triangles mark selected GPS sites KARR, ALIC, TOW2.

Fig. 3. The relative density of slips of phase (L) and group (P) GPS delay measurements $Q(t)$ during the solar radio burst on December 13, 2006; GEONET, Japan; L_1, L_2—(b), (a); and P_1, P_2—(d), (c), respectively. GPS signal parameters registered by TRIMBLE-5700 receivers (thin black lines) and by TRS-LEGACY receivers (thick gray lines). For TRS-LEGACY parameters L_1 and P_1 number of slips $Q(t) = 0$ during whole duration of radio burst.

was entirely absent. The measurement slip of L_2 and P_2 implies an impossibility of precise positioning in the dual-frequency mode; hence an incorrect determination of co-ordinates is possible in single-frequency mode. However, positioning in general is impossible if the signal at one of the GPS frequencies is not registered at all (Hofmann-Wellenhof *et al.*, 1992).

We also defined the corresponding maximum values $W_{\max}\%$ and $Q_{\max}\%$. The time resolution of the $W(t)$ dependence, 30 s, allowed us to compare in detail the $W(t)$ and $Q(t)$ values with those of the solar radio emission flux. We obtained data for all LOSs with an elevation angle θ between the direction along the LOS and terrestrial surface at the reception site of over $5°$.

4. Results

Figure 1(e) illustrates the process of registering the 30-s count omission for different PRN and selected GPS sites—KARR, ALIC, TOW2—located near sunlit points corresponding to 02:30 and 03:30 UT (Fig. 2, region R_3, Australia). Each time dependence of the elevation angle $\theta(t)$ is labeled with the GPS site and PRN name; empty time
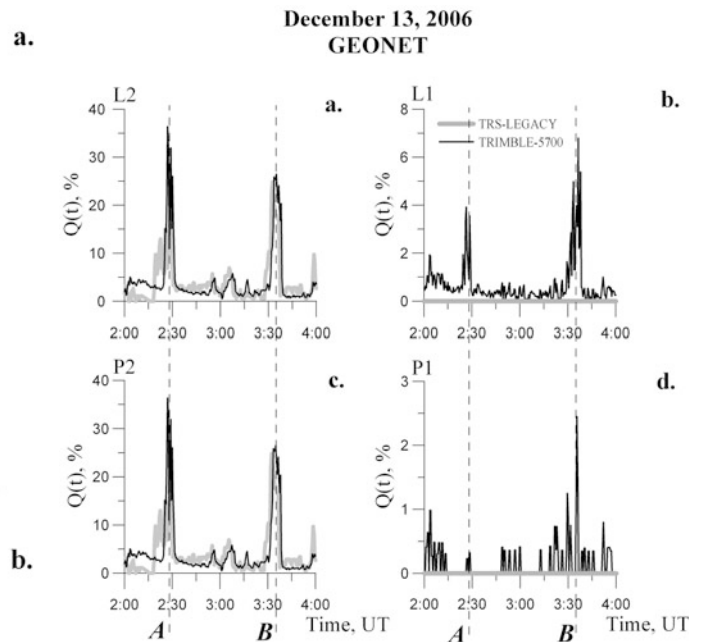
intervals correspond to count omissions.

One can see that for a low elevation angle $\theta < 30°$ the count omissions coincide with the impulse SRB during periods A and B (ALIC-01, ALIC-13, ALIC-27, KARR-13, KARR-27, TOW2-01). There are no count omissions for a high elevation angle θ (ALIC-20, KARR-20).

Figure 1 shows the dependence of count omissions in GPS measurements upon the Sun zenith angle χ during the 2006 December 13 SRB. The total count omissions $W(t)$ for all registered PRN are presented in panel (b) for region R_1 (black line, $80° > \chi > 90°$; $n = 51$), for region R_0 (thick gray line, $0° > \chi > 90°$; $n = 587$ GPS sites), and for region R_3 (gray line, $0° > \chi > 10°$; $n = 119$). The maximum $W_{\max}$ values of over 62% and 18% were recorded for $0° > \chi > 10°$, and $80° > \chi > 90°$, respectively. There was a wide range of zenith angles χ for the entire region R_0, but even for this region the maximum $W_{\max}$ values exceeded 37%, since the zenith angle χ did not exceed $50°$ for most of the GPS world network sites.

Figure 1(c) and (d) give the $W(t)$ time-dependences for satellites with selected PRN registered from 02:15 to 03:45 UT. Maximum $W_{\max}$ values for region R_0 can be as high as 50% (panel (c)) and 48% (PRN28, $n = 16$; and PRN13, $n = 43$, respectively). In region R_2 (panel (d), $\chi \sim 60°$), $W_{\max}$ is 19% and 8% (PRN22, $n = 405$; and PRN13, $n = 255$, respectively).

A sharp increase in count omissions completely coincides with the impulse SRB not only during periods A and B, but also, to a lesser extent, at 02:45–03:20 UT (Fig. 1). Comparison of the time dependence of count omissions $W(t)$ for the high zenith angle $0° > \chi > 10°$ to that for

the intensity of RHCP radio emission $F(t)$ at frequencies 1 GHz and 2 GHz demonstrate a close similarity between these dependences (Fig. 1(a, b)). It is also necessary to note that the threshold ε, at which GPS receiver failures occur at high zenith angle, does not exceed 20,000 sfu (as indicated by a horizontal line in panel (a)).

A comparison between different types of GPS receivers' response to wideband solar radio emission impact is of great interest. The dense network of GEONET GPS receivers, equipped with 1200 TRIMBLE-5700 and 25 TRS-LEGACY receivers, is best suited for this purpose. Since the entire network is expanded over a rather small area, all the receivers were under similar influence of the solar radio noise emission during the extreme solar activity on December 13, 2006. Figure 3 presents the relative density $Q(t)$ of measurement slips for the L_1, P_1, L_2, P_2 parameters registered by TRIMBLE-5700 (black lines) and TRS-LEGACY receivers (thick gray lines) on December 13, 2006. It is obvious that significant measurement slips for the main GPS signal parameters were registered by TRIMBLE-5700 receivers not only at the auxiliary frequency $f_2(L_2)$, but at the basic GPS frequency $f_1(L_1)$ as well. Nevertheless, significant measurement slips for the main parameters were detected by TRS-LEGACY receivers at the auxiliary frequency f_2 only. For TRS-LEGACY, the number of L_1 and P_1 slips was nil during the entire radio burst.

5. Discussion

There are some peculiarities in the time dependencies of count omissions and measurement slips for GPS-signal parameters we obtained:

5.1. Count omissions in GPS measurements increase as the line-of-sight elevation angle decreases. A monotonous reduction in signal level is associated with increasing satellite-to-receiver distance. Under usual conditions, additive noise in ~40 dB is below the level of signals, as a result of correlation processing of broadband signal in the receiver (Hofmann-Wellenhof *et al.*, 1992; ICD-200c). During powerful solar radio bursts, noise level at low elevation is higher than the signal, which causes failures in phase tracking of the GPS signal. Besides, according to the said mechanism, the dependence of density of the maximum count omissions is not proportional to the maximum radio emission power. It is likely to be determined by the signal-to-noise ratio threshold that may differ for different GPS receivers.

5.2. The GPS measurement count omissions at the auxiliary frequency f_2 essentially exceed those for the basic GPS frequency f_1. A lower signal/noise ratio at f_2 is primarily due to the fact that the f_2 power at the GPS satellite transmitter output is 6 dB less than that of the basic frequency f_1 with the C/A code (ICD-200c). Similar correlations of the effective radiated power of f_1 (30 watt) and f_2 (21 watt) signals are also typical of the Russian GLONASS system (Perov and Kharisov, 2005).

Phase tracking slips of the f_2 GPS signal may also be caused by lower signal/noise ratio when we use commercial noncoded receivers for f_2 installed at the global GPS network stations. These receivers have no access to the military "Y" code, and have to use the noncoded or semi-noncoded mode of reception. As a result, the signal/noise

ratio at f_2 is, at best, 13 dB lower than the mode of fully coded reception. Thus, the difference in signal powers at f_1 and f_2 for commercial receivers may exceed 10 dB, which may lead to a slip density increase at f_2 owing to the influence of additive interference, but different types of GPS receivers respond differently to this interference.

5.3. The maximum values of $W(t)$ for the time interval *A* are lower than those for *B*, while the radio flux $F(t)$ is also strong enough for both. It is quite natural, since strong bursts of solar radio emission at two GPS frequencies occurred simultaneously only during the time interval *B*, not *A* (Fig. 1(a)). Therefore the probability of the GPS count omissions is higher for the time interval *B* than for *A* (see Section 2).

5.4. The maximum values of $Q_{max}\%$ for L_2 and P_2 for TRIMBLE-5700 receivers for the time interval *A* are higher than those for *B*, while the opposite is true for the L_1 and P_1 parameters. On the other hand, the maximum values of L_2 and P_2 TRS-LEGACY receivers for the time interval *A* are lower than those for *B*. The main reason for this discrepancy are different characteristics of hardware and software components in different GPS receivers.

5.5. Besides, the maximum values $Q_{max}\%$ of all L_1, P_1, L_2, P_2 parameters are higher than those of count omissions $W_{max}\%$. It is quite natural, since $W(t)$ is registered for the count omission only, whereas $Q(t)$ includes not only the count omission, but also the measurement slips of each of the L_1, P_1, L_2, P_2 parameters (Section 2).

6. Conclusion

We found that high-precision GPS positioning on the entire sunlit side of the Earth was partially disrupted during the extreme solar-radio burst on December 13, 2006, for more than 12–15 min; a high level of GPS slips resulted from wideband solar radio noise emission. Our results agree with data obtained recently for the extreme solar radio burst on December 6, 2006 (Cerruti *et al.*, 2006a, b; Afraimovich *et al.*, 2007; Carrano *et al.*, 2007; Carrano and Bridgwood, 2008; Kintner, 2008).

We confirmed the results obtained by Carrano *et al.* (2007) in that GPS failure does depend on Sun zenith angle χ. An increase in count omissions at high zenith angles χ (Fig. 1) testifies to the solar origin of interference (noise) at two GPS frequencies. A growing number of failures with increasing zenith angle is caused by an increase in atmospheric losses.

We agree also with the conclusion by Chen *et al.* (2005). Direct interference from SRB is not usually considered as a potential threat to GPS signal tracing, since the flux density of most bursts is below the GPS f_1 frequency threat threshold of 40,000 sfu, proposed by Klobuchar *et al.* (1999). However, analysis by Chen *et al.* (2005) revealed that a much lower threshold (4,000–12,000 sfu) should be adopted for codeless or semicodeless dual-frequency GPS receivers. For SRB on December 13, 2006, the threshold ε, at which GPS receiver failures occur at high zenith angle, does not exceed 20,000 sfu (as indicated by a horizontal line on Fig. 1(a)).

A more detailed analysis of space distribution of GPS performance slips caused by strong solar radio bursts will

be the subject of our future works. There are other dense GPS networks, for example, the permanent Korean GPS Network, KGN (Jin and Park, 2007). The accurately unified national GPS network with more than 2500 stations, named "National 2000' GPS Control Network", has been established by integrating the existing six nationwide GPS networks of China (Yuanxi *et al.*, 2007). A similar analysis should be made for GPS failures during the 2006 December 13 powerful solar radio burst in the said regions.

Our results provide a serious basis for revising the role of space weather factors in the functioning of modern satellite systems and for taking a more thorough account of these factors, in practice. Similar failures in the functioning of satellite navigation systems (GPS, GLONASS, European system GALILEO) may be fatal to operating safety systems as a whole, leading to great financial losses. Another important conclusion of our investigation is that continuous calibrated monitoring of the solar radio emission flux level by a large number of solar radio spectrographs allows solar radio noise level in the range of GPS-GLONASS-GALILEO frequencies to be estimated. Indeed, strong solar radio bursts can be applied as a global and free tool for testing satellite broadband radio systems including GPS. We agree with this conclusion by Gary (2008): "As our society becomes ever more dependent on wireless technology, the effects of solar radio bursts can be expected to appear more often. Mission-critical systems should be designed with solar radio emission in mind. A warning system based on an improved set of world-wide instrumentation could be implemented at relatively low cost, taking advantage of new technology that allows broadband digital signal measurements. Ultimately, such extreme flux density bursts need to be studied at high spatial resolution in order to better understand the conditions leading to their occurrence, and ultimately to be able to predict such events".

References

Afraimovich, E. L., GPS global detection of the ionospheric response to solar flares, *Radio Sci.*, **35**(6), 1417–1424, 2000.

Afraimovich, E. L., E. A. Kosogorov, and L. A. Leonovich, The use of the international GPS network as the global detector (GLOBDET) simultaneously observing sudden ionospheric disturbances, *Earth Planets Space*, **52**(11), 1077–1082, 2000.

Afraimovich, E. L., O. S. Lesyuta, I. I. Ushakov, and S. V. Voeykov, Geomagnetic storms and the occurrence of phase slips in the reception of GPS signals, *Ann. Geophys.*, **45**(1), 55–71, 2002.

Afraimovich, E. L., G. A. Zherebtsov, and G. Ya. Smolkov, Total failure of GPS during a solar flare on December 6, 2006, *Doklady Earth Sci.*, **417**(8), 1231–1235, 2007.

Asai, A., H. Hara, T. Watanabe, Sh. Imada, T. Sakao, N. Narukage, J. L. Culhane, and G. A. Doschek, Strongly blueshifted phenomena observed with Hinode/EIS in the 2006 December 13 solar flare, *Astrophys. J.*, **684**, 2008 (in press). http://solar.physics.montana.edu/cgi-bin/eprint/index.pl?entry=7249, 2008-06-05 23:36 (submitted).

Carrano, C. S. and C. T. Bridgwood, Impacts of the December 2006 solar radio bursts on the performance of GPS, *Presented at the 12th International Ionosphere Effects Symposium, Alexandria*, VA, May 13–15, 2008.

Carrano, C. S., K. M. Groves, and C. T. Bridgwood, Effects of the December 2006 solar radio bursts on the GPS receivers of the AFRL-SCINDA network, *Proceedings of the International Beacon Satellite Symposium*, edited by P. H. Doherty, Boston College, June 11–15, 2007.

Cerruti, A. P., P. M. Kintner, D. E. Gary, L. J. Lanzerotti, E. R. de Paula, and H. B. Vo, Observed solar radio burst effects on GPS/WAAS carrier-to-noise ration, *Space Weather 4*, S10006, doi:10.1029/2006SW000254, http://gps.ece.cornell.edu/, 2006a.

Cerruti, A. P., P. M. Kintner, D. E. Gary, and L. J. Lanzerotti, Direct observations of GPS L1 signal-to-noise degradation due to solar radio bursts, *Eos Trans. AGU*, **87**(36), Jt. Assem. Suppl., 2006b.

Chen, Z., Y. Gao, and Z. Liu, Evaluation of solar radio bursts' effect on GPS receiver signal tracking within International GPS Service network, *Radio Sci.*, **40**, RS3012, doi:10.1029/2004RS003066, 2005.

Gary, D. E., Cause and extent of the extreme radio flux density reached by the solar flare of 2006 December 06, presented at *the 12th International Ionosphere Effects Symposium*, Alexandria, VA, May 13–15, 2008.

Hofmann-Wellenhof, B., H. Lichtenegger, and J. Collins, *Global Positioning System: Theory and Practice*, 327 p., Springer-Verlag Wien, New York, 1992.

Interface Control Document: ICD-200c, http://www.navcen.uscg.mil/pubs/gps/icd200/.

Jin, S. and J.-U. Park, GPS ionospheric tomography: A comparison with the IRI-2001 model over South Korea, *Earth Planets Space*, **59**(4), 287–292, 2007.

Kintner, P. M., An overview of solar radio bursts and GPS, IES 2008, presented at *the 12th International Ionosphere Effects Symposium*, Alexandria, VA, May 13–15, 2008.

Klobuchar, J. A., J. M. Kunches, and A. J. Van Dierendonck, Eye on the ionosphere: Potential solar radio burst effects on GPS signal to noise, *GPS Solutions*, **3**(2), 69–71, 1999.

Kubo, M., T. Yokoyama, Yu. Katsukawa *et al.*, Hinode observations of a vector magnetic field change associated with a flare on 2006 December 13, *Publ. Soc. Jpn.*, **59**, S779–S784, 2007.

Perov, A. I. and V. N. Kharisov, *GLONASS: principles of construction and functioning*, 720 p., Moscow, 2005 (in Russian).

Su, Yu., L. Golub, A. Van Ballegooijen *et al.*, Evolution of the sheared magnetic field of two X-class flares observed by Hinode/XRT, *Publ. Soc. Jpn.*, **59**, S785–S791, 2007.

Yuanxi, Y., T. Yingzhe, C. Chuanlu, W. Min, Z. Peng, W. Xiaorui, S. Lijie, and Z. Zusheng, National 2000' GPS control network of China, *Prog. Nat. Sci.*, **17**(8), 983–987, 2007.

E. L. Afraimovich (e-mail: afra@iszf.irk.ru), V. V. Demyanov, and G. Ya. Smolkov